

# 2023 | 637

## Simulation based layout of a highly efficient aftertreatment system for a large diesel engine

Emission Reduction Technologies - Exhaust Gas Aftertreatment Solutions

**Thomas Kammerdiener, AVL List GmbH**

Hannes Noll, AVL List GmbH  
Gareth John Estebanez, AVL List GmbH  
Ramin Mehrabian, LEC GmbH  
Christoph Redtenbacher, LEC GmbH  
Hendrik-David Noack, Umicore AG & Co. KG  
Alain Ristori, Umicore AG & Co. KG

---

This paper has been presented and published at the 30th CIMAC World Congress 2023 in Busan, Korea. The CIMAC Congress is held every three years, each time in a different member country. The Congress program centres around the presentation of Technical Papers on engine research and development, application engineering on the original equipment side and engine operation and maintenance on the end-user side. The themes of the 2023 event included Digitalization & Connectivity for different applications, System Integration & Hybridization, Electrification & Fuel Cells Development, Emission Reduction Technologies, Conventional and New Fuels, Dual Fuel Engines, Lubricants, Product Development of Gas and Diesel Engines, Components & Tribology, Turbochargers, Controls & Automation, Engine Thermodynamics, Simulation Technologies as well as Basic Research & Advanced Engineering. The copyright of this paper is with CIMAC. For further information please visit <https://www.cimac.com>.

## **ABSTRACT**

This paper focuses on the development of an exhaust aftertreatment system for a ~2 MW high-speed diesel engine capable of reaching emission levels significantly below current Stage V (EU Regulation 2016/1628) or Tier 4 standards (U.S. Environmental Protection Agency, 40 CFR). A development target of ~97% NO<sub>x</sub> conversion was set in the ISO 8178 C1 8-mode test schedule. To meet this target, the aftertreatment system utilizes SCR-based NO<sub>x</sub> reduction in combination with a diesel oxidation catalyst (DOC) and a diesel particulate filter (DPF). For system definition, a simulation study was performed using characteristics of advanced catalyst formulations. The simulation activities focused on the prediction of gaseous pollutant emissions, specifically nitrogen oxide emissions (NO<sub>x</sub>, N<sub>2</sub>O). A 1D simulation model was set up in AVL CRUISE™ M covering all relevant catalytic reactions, thermal behavior, and pressure loss of the aftertreatment system. The system was optimized through simulation to fulfill ultra-low emission targets and the selected catalysts were procured for hardware testing. Eventually, the actual aftertreatment system was tested in a measurement campaign on a multicylinder engine system test bed. The measurement data obtained in the testbed campaign is in good agreement with predictions from the simulation phase and the achievement of the project targets was confirmed.

## 1 INTRODUCTION

Diesel engines have held a dominant position for many decades in the large engine market. Their high-power density and efficiency combined with proven robustness of the combustion process and excellent transient capability together with widespread availability of diesel fuels and heavy fuel oils led to their predominant market position. Due to increased environmental awareness and the implementation and tightening of pollutant emission limits around the globe, focus will shift towards development of clean, ultra-low emission systems to retain competitiveness and market viability. Especially nitrogen oxide (NO<sub>x</sub>), particle-mass (PM) and particle-number (PN) emissions of current systems must be significantly reduced to ensure compliance with future legislative scenarios. Efficient exhaust aftertreatment systems must be introduced for the large engine sector to achieve these emission targets.

The aim of the presented project was to develop an SCR based exhaust aftertreatment system (EAS) for large high-speed diesel engines to meet ultra-low emission requirements (NO<sub>x</sub>, PM, PN, HC) in legislation cycles (e.g., ISO 8178-4:2020 Part 4 [1]) and in real operation. The following tailpipe emission targets, derived from progressive CARB Tier 5 locomotive standards [2], Stage V set by European Union [3] limits and other scenarios (e.g., TA Luft 2017 [4] / 44. BImSchV [5]), were defined:

- NO<sub>x</sub><0.25 g/kWh
- PM<10 mg/kWh
- PN<sub>23</sub><1x10<sup>12</sup> #/kWh
- HC<30 mg/kWh
- CO<0.8 g/kWh

An EAS demonstrator system was designed, installed, and tested on one cylinder bank of a V12 diesel engine with a rated power of ~2 MW and a NO<sub>x</sub> engine out emission level of around 10 g/kWh.

The ISO 8178 8-mode test schedule (Type C1) [1]– in the following referred to as NRSC (non-road-stationary-cycle) – was selected as the test cycle to investigate the EAS emission reduction potential in a broad operating range. An overview of the obtained results was already presented in [6].

All results shown in this paper are related to 6 cylinders respectively one bank of the V12 engine.

The work was carried out in a consortium consisting of three partners. LEC GmbH (*Graz, Austria*) provided the test facilities and was responsible for system integration and execution of

the test program on their multicylinder engine (MCE) system test bed. Umicore Denmark ApS (*Hoersholm, Denmark*) provided the catalysts and filter components required for build-up of the EAS. In addition, Umicore supported the project with an EAS pre-layout based on their know-how and experience with industrial and stationary applications. AVL List GmbH (*Graz, Austria*) provided engineering support in the form of simulation-based system validation and onsite support during the test campaign. The test campaign was executed using fresh, degreened catalyst and filter components. Through simulation with the EAS model developed in AVL CRUISE™ M, the system performance under aged conditions can be predicted.

In this paper, special focus is placed on the simulation-based EAS layout and validation. The simulation methodology is explained, the simulation results are correlated to experimental results obtained in the measurement phase of the project and a prediction for system performance in aged condition is given. Simulation activities are limited to performance prediction in view of gaseous emission constituents, while focussing especially on nitrogen oxide emissions (NO<sub>x</sub> and N<sub>2</sub>O). PM and PN emissions are not discussed in the paper at hand.

## 2 METHODOLOGY AND BOUNDARY CONDITIONS

The project was carried out in three main phases. First, the EAS arrangement as well as catalyst and filter specifications were pre-defined based on previous experiences to meet the defined emission targets. The selected EAS layout consists of a diesel oxidation catalyst (DOC), a diesel particulate filter (DPF) and a selective catalytic reduction system (SCR).

In the next phase an aftertreatment model was set up in the AVL simulation environment CRUISE™ M based on catalyst performance data provided by Umicore. The boundary conditions and engine out data required for the aftertreatment simulation was derived from available experimental data and 1D engine simulations performed by LEC. The objective of this modelling phase was to confirm the feasibility of target achievement with the selected catalysts by a system simulation approach. Moreover, a black-box model was developed in the AVL CRUISE™ M software for 1D model-based optimization of the overall system in a coupled engine and EAS model environment at LEC.

Afterwards, the detailed design of the specified EAS and the required measurement systems for demonstration on the MCE system test bed in combination with a 2 MW diesel engine was performed. Finally, the EAS was procured and installed at the test bed and the experimental investigations with detailed analyses of the overall system and the sub-systems were executed.

## 2.1 Engine specifications and test cycle

A 12-cylinder V60° 2 MW diesel engine was the basis for the design and demonstration of the EAS at the LEC system test bed. The engine is based on a J612 gas engine from INNIO Jenbacher that was converted to a diesel engine by LEC. The main engine specifications are summarized in Table 1.

Table 1: Diesel engine specifications

Number of cylinders	12
Cylinder arrangement	V 60°
Bore	190 mm
Stroke	220 mm
Displacement (cylinder)	6.24 dm <sup>3</sup>
Total displacement	74.9 dm <sup>3</sup>
Nominal speed	1500 1/min
Mean piston speed	11 m/s (1500 1/min)

The engine was calibrated to achieve a brake-specific NO<sub>x</sub> (BSNO<sub>x</sub>) emission level of 10 g/kWh in the NRSC. This cycle was consequently also used for the evaluation of the EAS. It represents a sequence of eight steady-state engine operation modes with different weighting factors. The eight cycle modes are defined by five different engine torque and three engine speed levels. The cycle modes and their corresponding weighting factors are shown in Figure 1. The weighting factors are used to calculate a cycle weighted mean value for every exhaust emission based on the emissions measured for each of the eight cycle modes, according to Equation 1 [1].

$$e_{gas} = \frac{\sum_{i=1}^{N_{mode}} (q_{mgas\ i} * WF_i)}{\sum_{i=1}^{N_{mode}} (P_i * WF_i)} \quad (1)$$

Equation 1 gives the mean cycle value ( $e_{gas}$ ) based on the mean emission mass-flow at each mode ( $q_{mgasi}$ ), the engine power of each mode ( $P_i$ ) and the corresponding weighting factor ( $WF_i$ ).

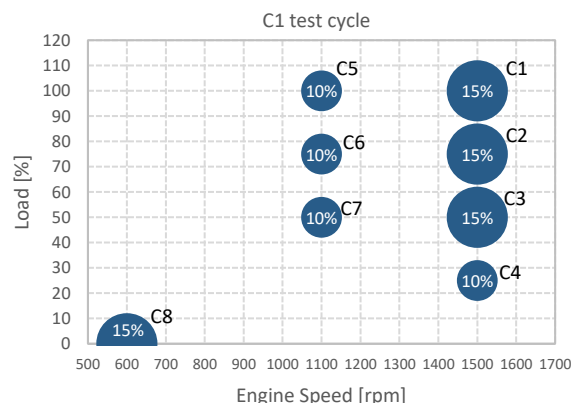


Figure 1: The eight cycle modes of the NRSC and their weighting factors in percentage

Brake-specific NO<sub>x</sub>, CO, and HC emissions as well as the exhaust temperature measured downstream of the turbocharger for each mode of the test cycle are summarized in Table 2. In each engine operation mode except for C8 (engine idling) the exhaust temperature is well above 250 °C which is generally a temperature threshold where high NO<sub>x</sub> conversion over an SCR catalyst is possible. CO and HC engine out emissions are mostly low and already close to the tailpipe target

Table 2: Engine out emissions and temperatures measured downstream of the turbocharger for each cycle mode of the NRSC

Cycle modes	T [°C]	BSNO <sub>x</sub> [g/kWh]	BSCO [g/kWh]	BSHC [g/kWh]
C1	412	9.8	0.07	0.04
C2	448	8.0	0.11	0.04
C3	358	10.0	0.15	0.05
C4	269	9.9	0.30	0.09
C5	372	12.0	0.05	0.03
C6	373	12.0	0.06	0.03
C7	384	10.0	0.10	0.04
C8	162	9.8	256	3.79
<b>Cycle mean value</b>		<b>10.07</b>	<b>0.36</b>	<b>0.04</b>

## 2.2 EAS design

Several EAS layouts were considered and evaluated at the beginning of the project. Eventually, it was decided to test an EAS consisting of a DOC, followed by a DPF and an SCR. This catalyst arrangement is well-proven in many commercial and industrial applications. The layout and instrumentation of the EAS installed on the LEC MCE system test bed is shown in Figure 2 (CAD rendering) and Figure 3 (EAS layout and instrumentation plan). In the demonstrator EAS, a cordierite DOC, a silicon carbide DPF and a corrugated vanadium SCR was used. No zone

coating at the end of the SCR or additional catalyst bricks to reduce NH<sub>3</sub> slip were integrated. The catalysts were selected and sized to minimize the backpressure of the EAS and its impact on engine performance. Catalysts and particle filters were built up by multiple block substrates arranged in grids of 4 x 4 (DOC & DPF) and 3 x 3 (SCR). They were delivered in fresh conditions and then degreased in the demonstrator system for 10 h at 500 °C EAS inlet temperature. The catalysts and particle filter specifications are listed in Table 3.

In addition, the maximum and minimum space velocities (SV) considering the different cycle modes of the NRSC are given in Table 3 for each catalyst.

Dosing of urea water solution (UWS) was realized over three nozzles, each with a maximum UWS mass flow rate of 10 kg/h. The three nozzles were positioned radially around the pipe upstream of the SCR with a 120° angle between them. Each nozzle was supplied by one pump from a common UWS tank. The mixing length for UWS decomposition was approximately two meters, with a static blade-mixer installed inside the pipe upstream of the SCR.

To minimize temperature loss from engine outlet to the SCR, the entire system was insulated. Insulation mats with a thickness of 140 mm filled with mineral wool (Power-teK WM640) were used.

Table 3: Catalysts and filters specifications and their space velocity ranges

Component	Volume [liter]	Cell density [CPSI]	PGM loading [g/ft <sup>3</sup> ]	Substrate type	Dimensions LxWxH [mm]	Number of bricks	Space velocity [1/h]
DOC	36	300	10	Cordierite	150x150x100	16	12400 – 123600
DPF	145	90	1	Silicon carbide	174x174x300	16	3100 – 30700
SCR	259	64	-	Corrugated vanadium	231x231x540	9	1700 – 17200

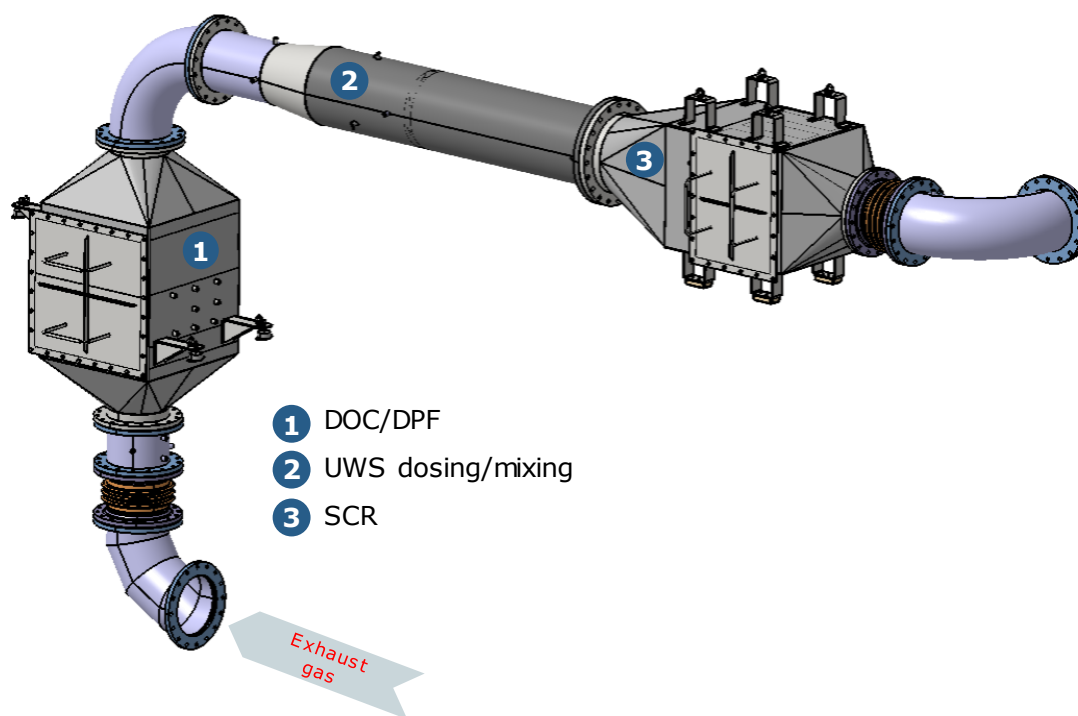


Figure 2: CAD rendering of the EAS (insulation mats not displayed)

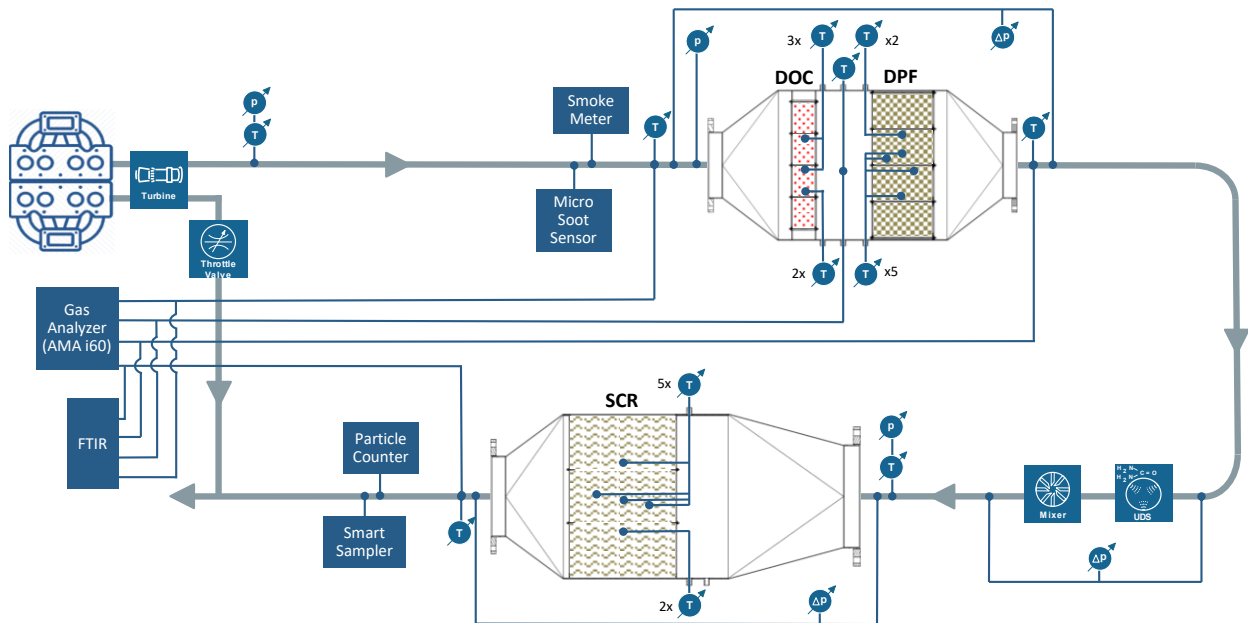


Figure 3: Layout and instrumentation of the EAS installed on the LEC MCE system test bed

### 2.3 Measurement procedure

As already described in section 2.1, the ISO 8178 C1 cycle [1] was applied for evaluation of the EAS. The UWS dosing was controlled in feed-forward mode based on the  $\text{NO}_x$  measurement upstream of the SCR. Dosing was activated when exceeding a temperature threshold of  $200\text{ }^\circ\text{C}$  upstream of the SCR, thus dosing was not active at engine idling, see Table 2 (NRSC mode C8).

The EAS was fully instrumented with thermocouples and pressure sensors upstream and downstream of each catalyst. In addition,  $0.5\text{ mm}$  thermocouples were inserted into the catalyst substrates to monitor the axial and radial temperature distribution in the substrate. Sampling positions for gas analysis were available upstream and downstream of each catalytic component. An AVL AMA i60 (for  $\text{CO}$ ,  $\text{CH}_4$ ,  $\text{THC}$ ,  $\text{NO}$  and  $\text{NO}_x$ ) and a SESAM i60 FTIR (for  $\text{CO}$ ,  $\text{C}_x\text{H}_y$ ,  $\text{NO}$ ,  $\text{NO}_2$ ,  $\text{N}_2\text{O}$  and  $\text{NH}_3$ ) were used for gas analysis. The AMA and FTIR could be switched independently between four sampling points. Thus, the performance of DOC, DPF, and SCR could be investigated thoroughly.

## 3 EAS MODEL SETUP

### 3.1 CRUISE™ M EAS model setup and simulation methodology

AVL CRUISE™ M was used to set up and parameterize a model of the aftertreatment system. In CRUISE™ M components like catalysts and pipes are modelled on 1D basis, which allows for

real time calculations. Physical effects like heat transfer, system backpressure as well as chemical reactions in catalysts and surface storage effects (e.g.,  $\text{NH}_3$  loading on the SCR, DPF soot loading) can be calculated.

For calculation of above-mentioned states and phenomena, the pipes, catalysts, and particle filter are divided into multiple cells (see Figure 4). Chemical reactions in catalysts are modelled based on an Arrhenius-approach. Pipes are modeled using a multi layer approach that allows to set different material properties for different layers (e.g., steel inner pipe surrounded by insulation material). The internal heat transfer from gas to the pipe is calculated based on Nusselt correlation for pipe flow while heat transfer to the environment is considered via convection and radiation effects.

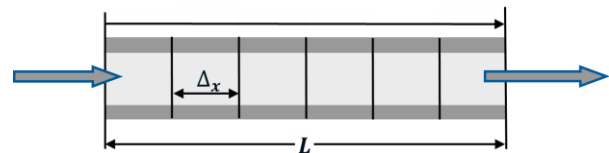


Figure 4: Scheme of multi-cell catalyst model in CRUISE™ M

The active components in the CRUISE™ M EAS simulation model reflect the system as presented in Figure 2 and Figure 3. The EAS model was set up in standalone mode. The required boundary conditions for the aftertreatment model, (i.e., engine out temperature, exhaust mass-flow and species composition as well as pressure downstream of the EAS) for verification simulations of the selected EAS hardware were obtained from

previous experiments and 1D engine simulations. Later, when the EAS was installed and experimental data for each cycle mode of the NRSC was available, the simulation boundary conditions have been fine tuned based on the actual MCE measurement results.

### 3.2 EAS thermal behaviour

Figure 5 shows the thermal behaviour of the simulation model compared to the measurement data in the NRSC. Catalyst and filter center substrate temperatures are plotted. The measurement data (black, dashed lines) is taken from discrete measurements of the different modes of the NRSC while the simulation (red, full lines) shows transient behaviour with 1200 s stabilization time per mode. This explains why the measurement data shows a step function while the simulation results provide transitions from each mode to the next. In stabilized conditions (after 1200 s operating time per mode) the model prediction is in good agreement with the measurement data. The maximum temperature deviation between measurement and simulation is below 10 K. The average temperature loss from DOC to SCR is 15-20 K in each mode of the NRSC (except for mode 8, engine idling).

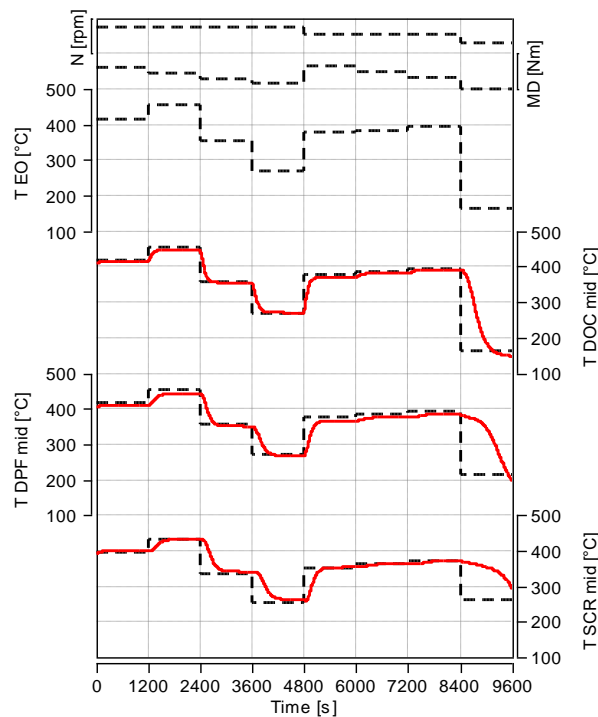


Figure 5: Catalyst and filter center temperatures in the NRSC; comparison of measurement data (black dashed line) and model prediction (red full line)

Furthermore, Figure 5 shows that in the 8<sup>th</sup> mode (idle operation) the system does not reach stable temperatures in the DPF or the SCR within 20 minutes. In all other transitions 20 minutes

stabilization time are sufficient to reach stable system temperatures in the SCR. This behaviour was also observed during the measurement campaign at the demonstrator system. It can be explained by the high thermal mass of the system in combination with low heat transfer under idle conditions (low exhaust mass-flow) leading to a slow cool-down of the system when changing to the idle mode at the end of the test procedure. Emissions in the NRSC should be measured after temperatures in the system have stabilized. To optimize the test program the assumption was made, that no emission conversion takes place any more after sufficient time in idle conditions, as the temperatures would eventually reach the engine out level of ~160°C. Therefore, the tailpipe emissions were assumed to be equal to the engine out emissions for calculation of the cycle weighted mean values.

### 3.3 EAS backpressure

Figure 6 shows the backpressure of the EAS in the different cycle modes of the NRSC. The backpressure of DOC, DPF and SCR including the mixing section as well as the total EAS backpressure are plotted. A maximum backpressure of 50 mbar is observed in the rated engine power point (C1). In general, the model predicted backpressure is well in line with measurement values presented in the CIMAC Tech Talk [6]. The measured values are presented in Figure 7 for comparison.

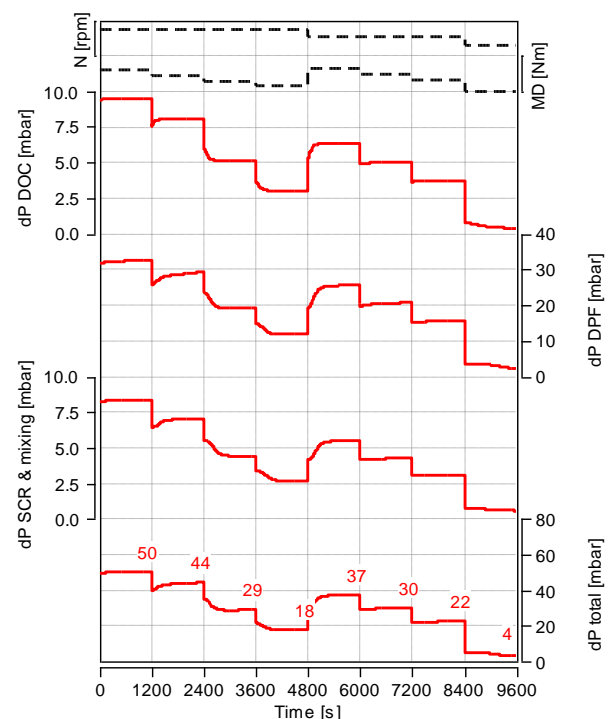


Figure 6: EAS backpressure in the ISO 8178 8-mode cycle; model prediction in red

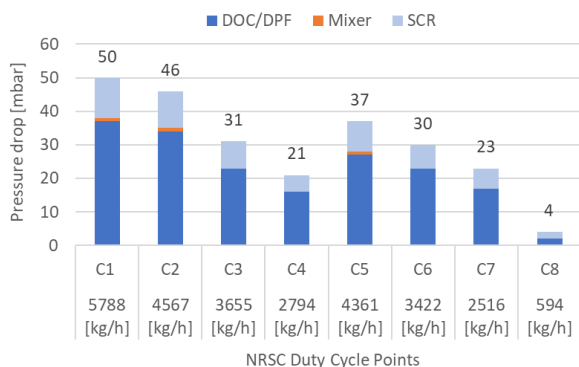


Figure 7: EAS backpressure in the ISO 8178 8-mode cycle; measurement data [1]

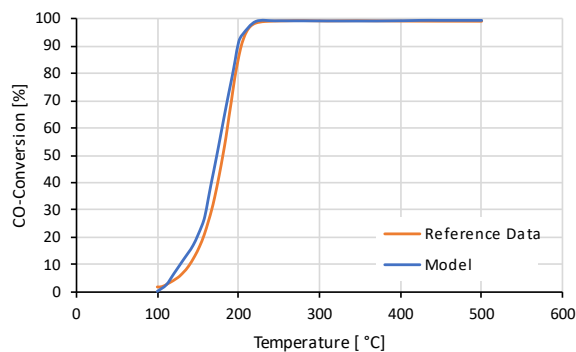


Figure 9: DOC CO conversion; model data in blue, reference performance data in orange;  $SV = 60000 \text{ h}^{-1}$ ,  $NO = 500 \text{ ppm}$ ,  $CO = 200 \text{ ppm}$ ,  $C_3H_6 = 60 \text{ ppm}$

### 3.4 Catalyst performance

Performance data of the selected catalysts was provided by Umicore for parameterization of the CRUISE™ M simulation model. The following diagrams summarize key performance indicators of DOC, DPF and SCR. In the following figures (Figure 8 - Figure 10) model data is plotted in blue, while the reference performance data is shown in orange color.

Figure 8 shows the temperature dependent DOC  $NO_2$  formation behaviour (molar  $NO_2/NO_x$  ratio). Except for a small deviation at around 200 °C the model prediction is in good agreement with the reference performance data, especially in the relevant NRSC temperature range of 260 to 450 °C.  $NO_2$  formation in the DOC and DPF is a key factor for the SCR  $NO_x$  conversion efficiency, as the  $NO_x$  conversion rate strongly depends on the available  $NO_2$  amount. Highest  $NO_x$  conversion can be achieved at a  $NO_2/NO_x$  ratio of 50% as the fast SCR reaction pathway is promoted.

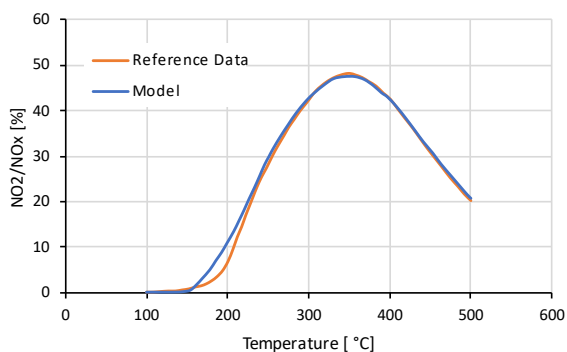


Figure 8: DOC  $NO_2$  formation; model data in blue, reference performance data in orange;  $SV = 60000 \text{ h}^{-1}$ ,  $NO = 500 \text{ ppm}$ ,  $CO = 200 \text{ ppm}$ ,  $C_3H_6 = 60 \text{ ppm}$

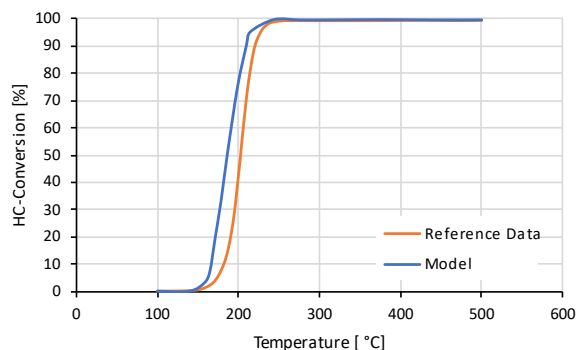


Figure 10: DOC HC conversion; model data in blue, reference performance data in orange;  $SV = 60000 \text{ h}^{-1}$ ,  $NO = 500 \text{ ppm}$ ,  $CO = 200 \text{ ppm}$ ,  $C_3H_6 = 60 \text{ ppm}$

Figure 9 and Figure 10 show the DOC CO and HC conversion rates over temperature. For both reactions the model slightly under-predicts the light-off temperature. This effect is more dominant for the HC oxidation. However, at temperatures above 200 °C, the model as well as the reference performance data show full CO conversion. Full HC conversion is reached at around 240 °C in both, the reference data, and the model prediction.

For the used DPF no performance data was available. Therefore, a reaction kinetic for a DPF with representative PGM loading from the AVL model database was used. The DPF model prediction is therefore directly compared to the NRSC measurement data. Figure 11 shows a comparison between the model prediction (red, full lines) and the measured  $NO_2/NO_x$  downstream of the DPF (black, dashed lines). The diagram includes the simulated  $NO_2/NO_x$  ratio downstream of the DOC as well as the DOC center temperature and space velocities over DOC and DPF. In general, the simulated  $NO_2/NO_x$  ratios are closely



matching the measurement values. A maximum deviation of  $\pm 3\%$  can be observed in the second and third cycle mode of the NRSC. Due to its low PGM loading, the  $\text{NO}_2/\text{NO}_x$  ratio increases on average by 1-2% over the DPF. Through appropriate sizing and layout of DOC and DPF the  $\text{NO}_2/\text{NO}_x$  ratio downstream of the DPF for all cycle modes is close to the optimum range of around 50% which enables highest  $\text{NO}_x$  conversion rates over the SCR. In the 8<sup>th</sup> cycle mode (engine idling) the majority of  $\text{NO}$  is oxidized to  $\text{NO}_2$  over DOC and DPF due to the low space velocity and still high substrate temperatures during the 20 min hold time. At stabilized temperatures of 160 °C the  $\text{NO}_2$  formation will drop significantly according to the trend previously indicated in Figure 8.

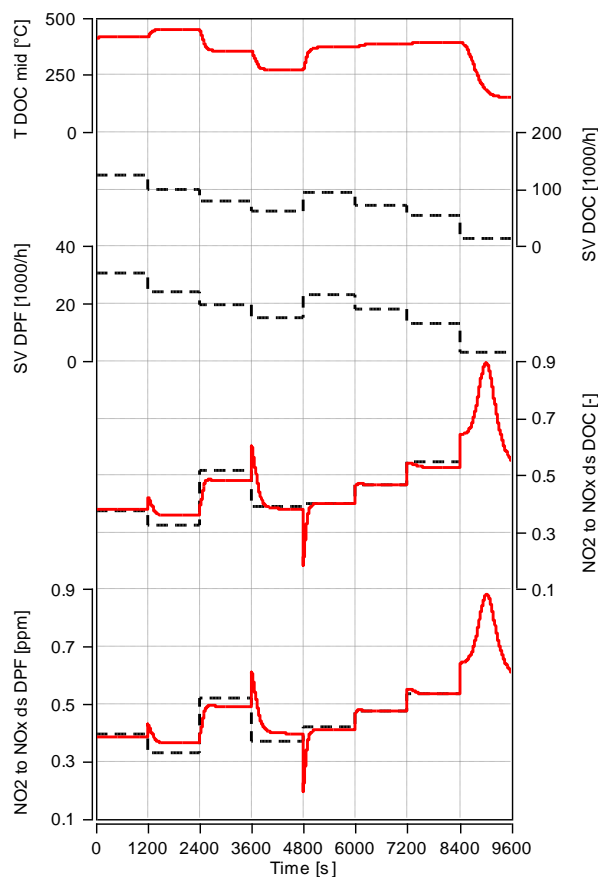


Figure 11:  $\text{NO}_2$  to  $\text{NO}_x$  ratio downstream DOC and downstream DPF in the ISO 8178 8-mode cycle; comparison of measurement data (black dashed line) and model prediction (red full line)

The DPF soot loading behaviour the NRSC and each separate mode was investigated with the simulation model. It could be confirmed that due to the high temperatures and high  $\text{NO}_2$ /soot ratio passive operation of the DPF is possible in the NRSC.  $\text{NO}_2$  borne soot regeneration in the DPF is sufficient to achieve a low, stabilized DPF soot loading during continuous operation in the NRSC as indicated in Figure 12. 20 min hold time per

mode of the NRSC were used in the soot loading simulation. The DPF soot loading reaches a stable level of around 0.2 g/l after 10 h continuous NRSC operation. Build-up of soot loading in the DPF is mainly observed in the C4 mode, while in other modes passive soot burn-off leads to a low overall soot loading.

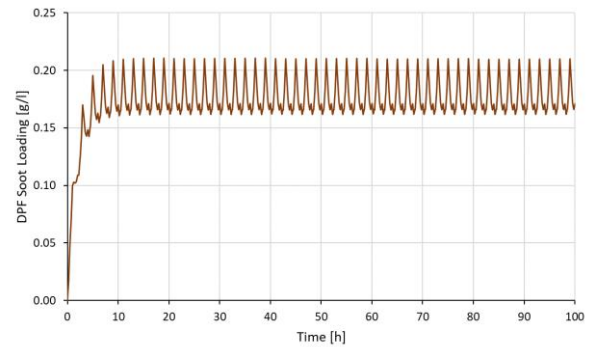


Figure 12: DPF soot loading over 100 h continuous NRSC operation (20 min hold time per mode)

For the SCR catalyst, Umicore provided performance data in fresh and aged conditions which is displayed in Figure 13. The diagram shows temperature dependent  $\text{NO}_x$  conversion rates for 25%  $\text{NO}_2/\text{NO}_x$  upstream of the SCR for 15000 and 20000  $\text{h}^{-1}$  space velocity. The data reflects a flow velocity and  $\text{NH}_3/\text{NO}_x$  maldistribution of 1% standard deviation. Full  $\text{NO}_x$  conversion is feasible at a space velocity of 15000  $\text{h}^{-1}$  in fresh condition in a broad temperature range while the conversion efficiency slightly drops towards higher space velocities and more severely under aged conditions. The aged data represents the SCR performance after 16000 h of operation in the load range of the NRSC considering thermal and chemical ageing effects (e.g., sulfur poisoning).

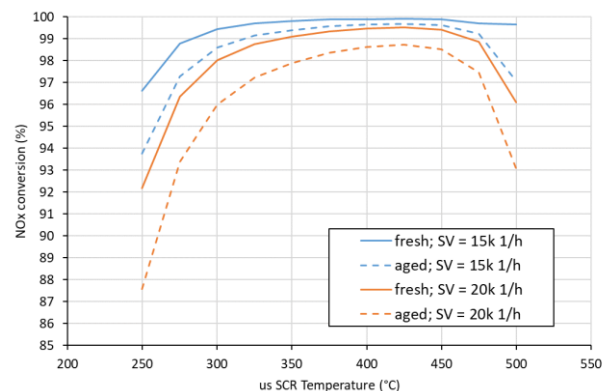


Figure 13: SCR  $\text{NO}_x$  conversion performance data (reference) in fresh (full lines) and aged (dashed lines) conditions for 15k and 20k  $\text{h}^{-1}$  space velocities; 25%  $\text{NO}_2/\text{NO}_x$ ; 500 ppm  $\text{NO}_x$ , 600 ppm  $\text{NH}_3$

The SCR reaction kinetic in the AVL CRUISE™ M simulation model was adjusted to match the

provided performance data at an  $\text{NO}_2/\text{NO}_x$  inlet ratio of 25 %. The reaction kinetic was built on an already existing Vanadium SCR model available in the simulation software, meaning that also the  $\text{NO}_x$  conversion dependency on the SCR inlet  $\text{NO}_2/\text{NO}_x$  ratio as well as the  $\text{N}_2\text{O}$  formation behaviour typical for a Vanadium SCR can be predicted by the model.  $\text{N}_2\text{O}$  is formed as a by-product during  $\text{NO}_x$  conversion, with Vanadium-SCR technology showing a low selectivity towards  $\text{N}_2\text{O}$  formation below 400°C.

Both, SCR  $\text{NO}_x$  conversion and  $\text{N}_2\text{O}$  formation of the simulation model are displayed in the following figures for the relevant temperature range of the NRSC. In fresh condition (Figure 14) the SCR model is slightly underpredicting the  $\text{NO}_x$  conversion rates at temperatures between 250 and 300 °C. In general, the  $\text{NO}_x$  conversion of the simulation model is in good agreement with the reference data for both space velocity levels. The model predicted  $\text{N}_2\text{O}$  formation shows the well-known trend for vanadium-based SCR with very low levels at temperatures lower than 400 °C followed by a sharp increase towards higher temperature.

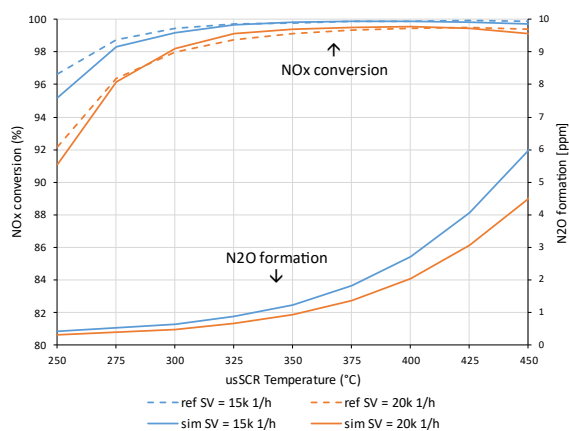


Figure 14: SCR  $\text{NO}_x$  conversion model prediction (full line) vs. reference data (dashed line) and  $\text{N}_2\text{O}$  formation model prediction in fresh conditions; 15k and 20k  $\text{h}^{-1}$  space velocities; 25%  $\text{NO}_2/\text{NO}_x$ ; 500 ppm  $\text{NO}_x$ , 600 ppm  $\text{NH}_3$

In aged condition (Figure 15), the SCR model fit to the reference data shows a similar trend as in fresh condition. A minor underprediction of  $\text{NO}_x$  conversion performance can be observed at temperatures below 300 °C. Additionally, the model  $\text{NO}_x$  conversion at 20000  $\text{h}^{-1}$  space velocity is lower than in the reference data. The  $\text{N}_2\text{O}$  formation behavior shows the same trend as in fresh conditions. Through ageing the SCR,

selectivity shifts towards a higher  $\text{N}_2\text{O}$  formation level and lower  $\text{NO}_x$  conversion rates.

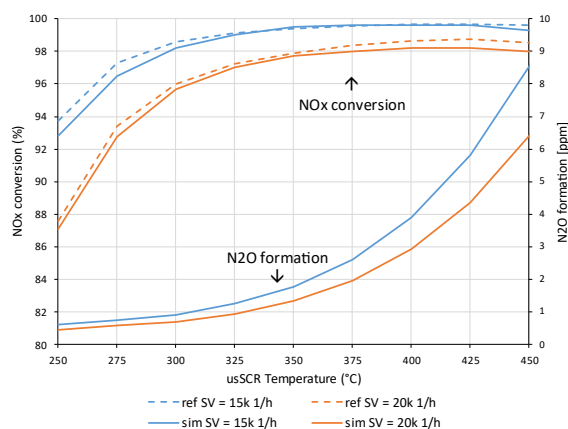


Figure 15: SCR  $\text{NO}_x$  conversion model prediction (full line) vs. reference data (dashed line) and  $\text{N}_2\text{O}$  formation model prediction in aged conditions; 15k and 20k  $\text{h}^{-1}$  space velocities; 25%  $\text{NO}_2/\text{NO}_x$ ; 500 ppm  $\text{NO}_x$ , 600 ppm  $\text{NH}_3$

### 3.5 Urea dosing strategy

A feed-forward dosing control strategy was applied in the simulation model and carried over to the test system. The dosed UWS quantity is calculated based on the  $\text{NO}_x$  engine out level. To achieve the NRSC tailpipe  $\text{NO}_x$  emission target of 0.25 g/kWh with approximately 10 g/kWh  $\text{NO}_x$  engine out, a cycle average SCR-efficiency greater than 97.5 % is required. To ensure highest  $\text{NO}_x$  conversion rates, ammonia to  $\text{NO}_x$  ratios (ANR) above the stoichiometric ratio were considered for the simulation-based concept verification. A demand ANR of 1.05 was set in the simulation model and was also targeted for the demonstrator system.

The used Vanadium SCR technology has a limited  $\text{NH}_3$  storage capacity that drops to almost zero at temperatures above 300 °C. Additionally, vanadium SCR shows a quick response to dosed  $\text{NH}_3$ , thus it works efficiently also without  $\text{NH}_3$  loading. Considering the high exhaust gas temperatures of the demonstrator engine and the characteristics of the Vanadium SCR,  $\text{NH}_3$  loading-based dosing control was not considered in the testing program.

## 4 VALIDATION OF THE SIMULATION MODEL

### 4.1 Experimental emission results

BSNO<sub>x</sub> tailpipe results and correlating SCR NO<sub>x</sub> conversion efficiencies are presented in Figure 16 for each single mode of the NRSC (C1-C8). The combined NRSC NO<sub>x</sub> emissions calculated according to Equation 1 as well as the cycle mean SCR efficiency are presented as the 9<sup>th</sup> dataset in the diagram. The presented NO<sub>x</sub> TP measurement values were achieved while limiting the NH<sub>3</sub> slip downstream of the SCR in all operating points to less than 50 ppm. Reduction of NH<sub>3</sub> emissions in this magnitude is feasible by using an ammonia slip catalyst downstream of the SCR which was not used in the test setup..

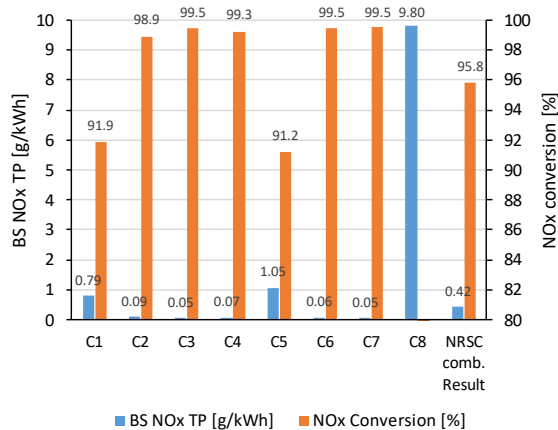


Figure 16: Measured BSNO<sub>x</sub> TP emissions & conversion rate per NRSC mode and combined NRSC value

The measured BSNO<sub>x</sub> TP in the C1 and C5 cycle modes are significantly higher than the measured TP emissions in other modes. This can be attributed to a malfunction of the dosing system leading to a limitation of the UWS dosing flowrate. Hence, sufficient NH<sub>3</sub> availability at these two cycle modes could not be reached. In both C1 and C5, the engine is operating at 100 % torque, leading to the highest exhaust mass-flow and consequently NO<sub>x</sub> flowrate among the NRSC modes. The limitations of the dosing system resulted in an ANR of approximately 0.9 for the C1 and C5 modes.

In all other NRSC modes high temperatures, favorable NO<sub>2</sub>/NO<sub>x</sub> ratios upstream the SCR, and low SCR space velocities lead to high NO<sub>x</sub> conversion rates. Due to low temperatures in the C8 cycle mode UWS dosing is not active. Consequently, no NO<sub>x</sub> conversion takes place over the SCR and tailpipe emissions are assumed to be on the same level as engine out emissions. NO<sub>x</sub> conversion rates ranging from 98.9 to 99.5 % were achieved. Due to high temperatures in the NRSC the set CO and HC tailpipe emission targets could

be fulfilled with the demonstrator system. Combined NRSC CO tailpipe emissions of 91 mg/kWh and combined HC tailpipe emissions of 15 mg/kWh were achieved in the NRSC [6].

### 4.2 Comparison of EAS model prediction and experimental results

Figure 17 shows the NRSC BSNO<sub>x</sub> simulation results with the SCR kinetic parameterized to the performance of the fresh catalyst compared to the measurement data from the MCE experiment.

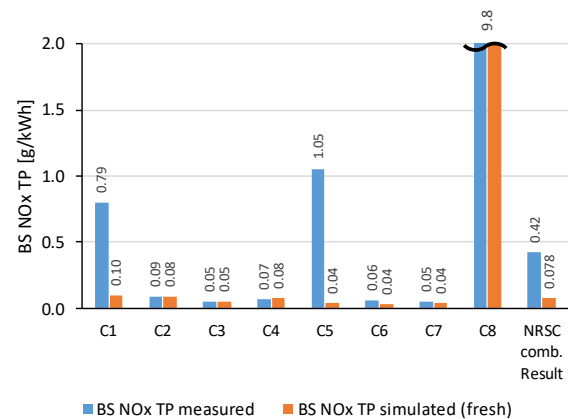


Figure 17: Comparison of BSNO<sub>x</sub> TP results from simulation and measurement in fresh conditions; single mode values and weighted mean NRSC value

As established in chapter 3.5, the ammonia to NO<sub>x</sub> ratio in the simulation was set to 1.05 for all NRSC modes. When comparing simulation to measurement, the higher UWS dosing in the simulation for modes C1 and C5 leads to significantly lower TP NO<sub>x</sub> emissions and consequently, higher NO<sub>x</sub> conversion rates. In all other cycle modes where the UWS dosing in the experiment was sufficient to achieve stoichiometric conditions, the model predicted values and the experimental data correlate well.

The higher measured NO<sub>x</sub> TP emissions from the MCE experiment in the C1 and C5 modes, result in a considerably higher combined cycle value compared to the model prediction. With 78 mg/kWh is the latter well below the development target of 250 mg/kWh. It means an overall NO<sub>x</sub> conversion efficiency of 99.2 % can be achieved the NRSC with the SCR in fresh condition. Although it is not discussed in detail in the following, the model predicted CO and HC emissions are well in line with the measurement values.

Figure 18 compares N<sub>2</sub>O TP emission results from the simulation model and the experimental investigations. The N<sub>2</sub>O formation over the SCR is strongly dependent on the exhaust temperature as shown in Figure 14 and Figure 15. Therefore, the

NRSC C2 mode shows the highest N<sub>2</sub>O emissions in both simulation and experimental investigations. In the C8 cycle mode (idle operation), no N<sub>2</sub>O emissions occur as urea dosing and therefore the SCR are not active.

The model predicts lower N<sub>2</sub>O emission values than measured on the demonstrator. This deviation can be explained by the chosen approach during model setup. As no N<sub>2</sub>O reference performance data for the used SCR catalyst was available, the model reflects the performance of the already available base Vanadium SCR kinetic from the CRUISE™ M database (parameterized to a different catalyst). In general, the trend observed in the measurement with increasing N<sub>2</sub>O formation towards increasing exhaust temperature is also reflected in the simulation result. The weighted mean NRSC BSN<sub>2</sub>O TP emission from simulation amounts to 21 mg/kWh while the one from the measurement is 27 mg/kWh. Usage of Vanadium-based SCR technology enables the achievement of a low N<sub>2</sub>O emission level in the NRSC which is especially important considering the high global warming potential of N<sub>2</sub>O. The cycle result for NH<sub>3</sub> for the measurement was 20 ppm with a peak of 50 ppm in the third operating mode of the test cycle. The simulated cycle result of 5 ppm with a peak of 29 ppm in the fifth load point is slightly lower than the measurement.

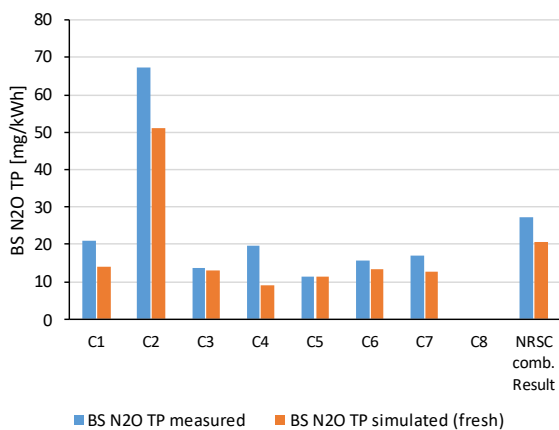


Figure 18: Comparison of BS N<sub>2</sub>O TP results from simulation and measurement in fresh conditions; single point and weighted mean NRSC results

## 5 EMISSION PREDICTION FOR THE AGED EAS

After validating the model with the experimental data, it was in a final step used to predict the NO<sub>x</sub> emissions under aged condition by utilising the SCR kinetic parameterized based on the aged SCR performance data.

A comparison between fresh and aged NO<sub>x</sub> emissions is given in Figure 19. In aged condition, the weighted mean NRSC simulation result is 260 mg/kWh. SCR ageing generally shows the biggest impact on NRSC modes with high engine load and exhaust temperature (modes C1, C2 and C5). A severe decrease of NO<sub>x</sub> conversion rates can also be observed in C4, which is the coldest mode of the NRSC. In the remaining modes, which lie in the sweet spot in view of temperature and SCR space velocity, a moderate increase of NO<sub>x</sub> TP emissions can be seen. The overall result indicates that with an aged SCR a conversion efficiency of >97 % can be reached in the NRSC.

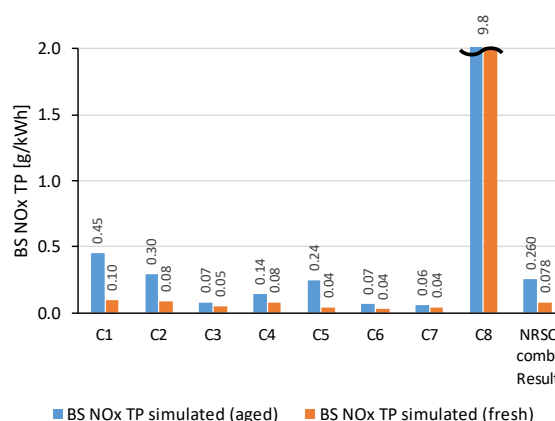


Figure 19: Comparison of BS NO<sub>x</sub> TP simulation results between fresh and aged SCR condition

## 6 CONCLUSION

An EAS for a ~2 MW large high-speed diesel engine was successfully designed and tested at the LEC MCE test bed system. Its compliance with stringent pollutant emission limits derived from proposed CARB Tier 5 and European Stage V legislation was proven.

An EAS simulation model was developed in AVL CRUISE™ M that represents the tested demonstrator system in view of thermal, backpressure and catalyst behaviour. Catalyst kinetics in the simulation model were parameterized based on performance data for the selected catalysts provided by Umicore. SCR performance data in fresh and aged condition was provided for the model setup. A good agreement between model prediction and measurement data could be achieved in view of NO<sub>x</sub> and N<sub>2</sub>O tailpipe emissions as well as for temperature and pressure losses along the EAS.

With the EAS model, a performance prediction for the entire NRSC load range can be provided. Results indicate that with fresh SCR catalyst

weighted mean NRSC NO<sub>x</sub> emissions of approximately 80 mg/kWh can be achieved, while the emission level under aged catalyst conditions is around 260 mg/kWh. Therefore, the NO<sub>x</sub> TP target of the project is successfully fulfilled. A prerequisite to achieve these progressive tailpipe emission levels is sufficient NH<sub>3</sub> dosing (ANR ≥1) as well as high NH<sub>3</sub> uniformity upstream of the SCR catalyst ensured by appropriate mixer design.

## 7 DEFINITIONS, ACRONYMS, ABBREVIATIONS

**ANR:** ammonia to NO<sub>x</sub> ratio  
**BS:** brake-specific  
**CPSI:** channels per square inch (catalyst cell density)  
**DOC:** diesel oxidation catalyst  
**DPF:** diesel particulate filter  
**EAS:** exhaust aftertreatment system  
**EO:** engine out  
**HC:** hydrocarbons (C<sub>1</sub>-basis)  
**MCE:** multi-cylinder engine  
**NO<sub>x</sub>:** nitrogen oxide (sum of NO and NO<sub>2</sub>)  
**PGM:** platinum group metals  
**PM:** particulate mass  
**PN:** particulate number  
**SCE:** single-cylinder engine  
**SCR:** selective catalytic reduction catalyst  
**SV:** space velocity  
**TP:** tailpipe  
**UWS:** urea water solution (32.5 % urea in water)

## 8 ACKNOWLEDGEMENTS

The authors would like to acknowledge the financial support of the "COMET - Competence Centers for Excellent Technologies" program of the Austrian Federal Ministry for Climate Action, Environment, Energy, Mobility, Innovation and Technology (BMK) and the Austrian Federal Ministry of Labor and Economy (BMAW) and the Provinces of Salzburg, Styria, and Tyrol for the COMET Centre (K1) LEC GETS. The COMET Program is managed by the Austrian Research Promotion Agency (FFG).

## 9 REFERENCES AND BIBLIOGRAPHY

- [1] ISO 8178-4:2020, "Reciprocating internal combustion engines — Exhaust emission measurement — Part 4: Steady-state and transient test cycles for different engine applications"
- [2] CARB Petitions U.S. EPA to Strengthen Locomotive Emission Standards, Petition and Cover Letter: April 2017 [https://ww2.arb.ca.gov/sites/default/files/2020-07/final\\_locomotive\\_petition\\_and\\_cover\\_letter\\_4\\_3\\_17.pdf](https://ww2.arb.ca.gov/sites/default/files/2020-07/final_locomotive_petition_and_cover_letter_4_3_17.pdf) accessed February 08, 2023.
- [3] Regulation (EU) 2016/1628 of the European Parliament and of the Council of 14 September 2016 on requirements relating to gaseous and particulate pollutant emission limits and type-approval for internal combustion engines for non-road mobile machinery, amending Regulations (EU) No 1024/2012 and (EU) No 167/2013, and amending and repealing Directive 97/68/EC, in: Official Journal of the European Union L 252/53, September 16, 2016.
- [4] Bundesministerium für Umwelt, Naturschutz und Reaktorsicherheit (2016): "Entwurf zur Anpassung der Ersten Allgemeinen Verwaltungsvorschrift zum Bundes-Immissionsschutzgesetz (Technische Anleitung zur Reinhaltung der Luft – TA Luft)"
- [5] 44. Verordnung zur Durchführung des Bundes-Immissionsschutzgesetzes "Verordnung über mittelgroße Feuerungs-Gasturbinen- und Verbrennungsmotoranlagen vom 13. Juni 2019 (BGBl. I S. 804), die durch Artikel 3 Absatz 1 der Verordnung vom 6. Juli 2021 (BGBl. I S. 2514) geändert worden ist
- [6] Mehrabian, R. et al., 2022. Optimized integration of a SCR-based aftertreatment system into a multicylinder, large diesel engine, presented at: *CIMAC Tech-Talks Special: Emissions Reduction (2)*.